Development of New Human Thermal Model based on Blood Flow Rate Measurements under Different Temperature Conditions

Tomonobu Goto[1,*], Daiki Terayama[2], Hiroto Sakamoto[3], Toshiyuki Hayase[1], Yoshifumi Saijo[1], Ryota Sugawara[1], Zhuoxi Niu[1]

[1]Tohoku University, Sendai, Japan
[2]Kajima Corporation, Tokyo, Japan
[3]Maeda Corporation, Tokyo, Japan
[*]*Corresponding email: t-goto@sabine.pln.archi.tohoku.ac.jp*

SUMMARY

In order to evaluate health risks under severe thermal environments, we are developing a new human thermophysiological model, which can predict not only body temperature but also blood pressure (BP) and blood flow rate (BFR). In the present study, we developed a sub-model (thermal network model) to simulate body temperature, and carried out subjective experiments under different ambient temperatures to collect reference data. The experiments indicated that human thermoregulatory ability in cold environments is weaker than that in hot environments. The experiments also showed that BFRs of limbs compose only small portions of total BFR but increase greatly with ambient temperature. On the other hand, our thermal network model could reproduce the trend of tympanic temperature and mean skin temperature. In addition, some numerical simulations showed that the BFRs of limbs are important for thermoregulation even if their portions are small, and besides, heat transfer along vessels is also important.

1 INTRODUCTION

Severe thermal environments cause human health problems, e.g. heat illness, cerebral stroke, heart attack, etc., and those incidences are increasing as the population ages in Japan (Ministry of the environment government of Japan, 2014; Tokyo metropolitan institute of gerontology, 2013). In the mechanism of them, changes in body temperature, blood pressure (BP) and blood flow rate (BFR) are key factors. For example, when people are exposed to hot environments, increase in skin blood flow rate is very important to prevent hyperthermia. But it also brings about decrease in BP and BFR to the vital organs, and cerebral ischemia or undue stress on heart can be caused (Ministry of the environment government of Japan, 2014). In another case, a sudden change of thermal environment cause a sudden change of BP, and consequently cerebral stroke or heart attack can be induced (Tochihara, 2012). Furthermore, those health problems are affected not only by thermal environments but also by individual behaviours (posture and activity level), physical constitutions (size, composition) and predispositions (pre-existing disorder, age, gender, heredity). That is to say, the risks of those health problems are attributed to the combined effects of those factors.

Numerical simulation with human thermophysiological model is one of the useful methods to evaluate the health risks induced by severe thermal environments. However, the conventional models cannot predict BP, and their BFR predictions are not sufficiently validated. Thus, no models are presently available to predict BP and BFR. One reason is that the conventional

models have been developed mainly for predicting body temperature. Another reason is that those values are difficult to measure, and hence little reference data have been available.

Our final goal is the development of a new human model, which can predict not only body temperature but also BP and BFR. Figure 1 shows the schematic of the developing model. It consists of two physical models, i.e. thermal network model and cardiovascular model, and a physiological model. The thermal network model is to simulate the heat transfer of a human body, and the cardiovascular model is to simulate the BP and BFR. The physiological model is to simulate the physiological regulation due to automatic nerve, e.g. vasodilation, vasoconstriction and perspiration. In our previous studies (Sakamoto et al., 2015; Goto et al., 2017), we had done some subjective experiments to collect reference data including BP and BFR under several experimental conditions where ambient temperature and body posture were varied. In addition, we had also developed the cardiovascular model (1.B in Figure 1), and confirmed that the developed cardiovascular model could reproduce the measured BP and BFR reasonably.

In the present study, we carried out some new subjective experiments to extend the reference data, and selected ambient temperature for the experiment parameter. Moreover, we developed the thermal network model (1.A in Figure 1) and tried to validate this model by comparing with the experiments.
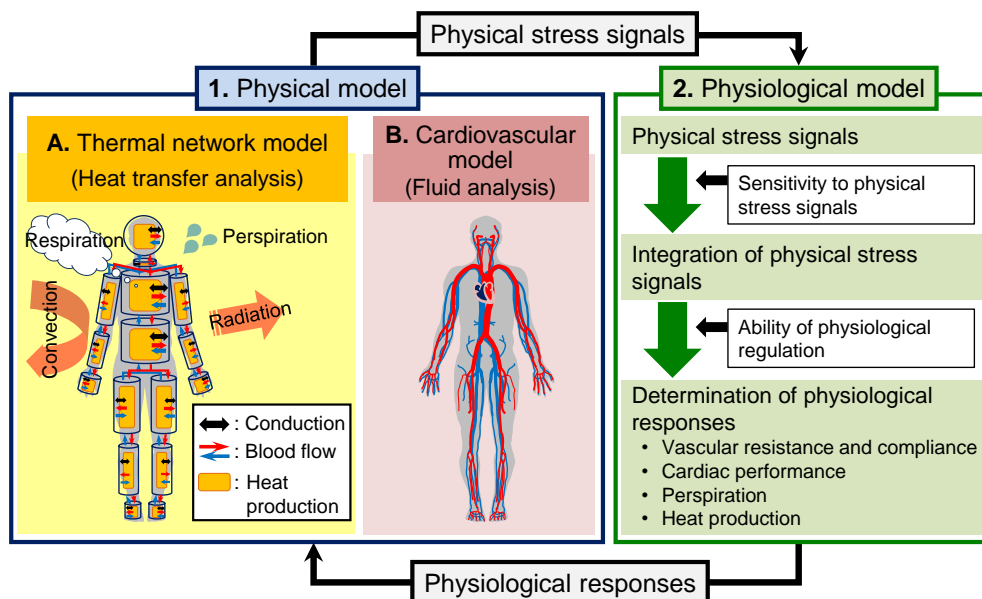

Figure 1. Schematic of new human thermophysiological model

2 METHODS
2.1 Subjective Experiments
The experiments were performed from August 2014 to December 2017, in a climate chamber at Tohoku University. A healthy young man participated as the subject. Tables 1 and 2 respectively show the experimental conditions and measurement items. The 28°C case was considered to be a thermally neutral and basic condition, while the other cases were colder and hotter conditions with different levels. Here, it should be noted that the present experiments were planned to measure the steady state human responses, despite the importance of unsteady responses on human health. Because we should well understand steady state responses and validate our simulation model for steady state conditions before unsteady state conditions.

The measurement items and points were numerous, and multiple measurements were important. Therefore, several experimental sessions were carried out for each experimental case, and the measurements were completed through those sessions. Figure 2 shows the schedule of an experimental session. The subject adapted to the experimental conditions during at least 30 min. After the adaptation period, arterial BFR, skin BFR and heat flux were sequentially measured at each point. An ultrasound imaging equipment (Aplio SSA-700A, TOSHIBA) and a laser speckle blood flowmeter (FLO-Lab, OMEGAWAVE) were used to measure the arterial BFR including cardiac output and skin BFR respectively. BP at upper arm and ankle were measured every 30 minutes, and body weight was measured at the beginning and end of the measurement period. The other items were measured continuously during the measurement period.

Table 1. Experimental conditions

Case	Air temperature and MRT	Humidity	Air velocity	Clothing insulation	Body posture
18°C	18°C	Not controlled	< 0.1 m/s	0.06 clo (under pants, short pants)	Supine
23°C	23°C				
28°C	28°C				
35°C	35°C				
40°C	40°C				

Table 2. Measurement items and points

| Measurement items	Measurement points
Arterial blood flow rate and cardiac output	Common carotid, Vertebral, External carotid, Internal carotid, Brachial, Radial, Ulnar (proximal side, distal side), Femoral, Deep femoral, Popliteal, Posterior tibial, Anterior tibial, Left ventricular outflow tract
Skin blood flow rate	Forehead, Neck, Chest, Back, Abdomen, Waist, Upper arm (front, back), Lower arm (front, back), Hand (palm, dorsum, finger), Thigh (front, back), Leg (front, back), Foot (sole, dorsum, toe)
Blood pressure	Upper arm, Ankle
Heart rate	Chest
Core temperature	Tympanum
Skin temperature	Forehead, Neck, Chest, Back, Abdomen, Waist, Upper arm, Lower arm, Hand, Thigh (front, back), Leg (front, back), Foot
Skin heat flux	Forehead, Neck, Chest, Back, Abdomen, Waist, Upper arm, Lower arm, Hand, Thigh (front, back), Leg (front, back), Foot
Metabolic rate	Whole body (oxygen consumption)
Perspiration	Whole body (weight loss)
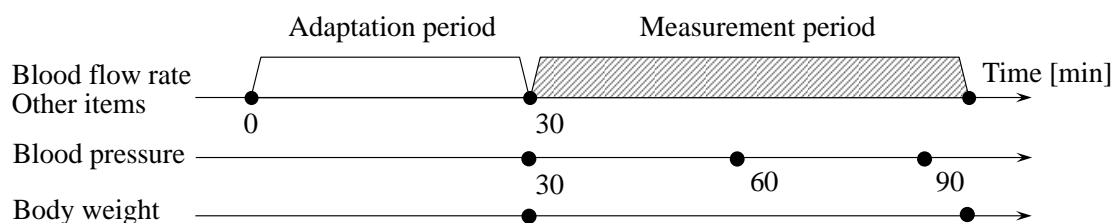
Figure 2. Schedule of experimental session

2.2 Numerical Simulation
We developed thermal network model, which is one of the physical models to be integrated in our new human thermophysiological model (Figure 1). This model was developed based on Stolwijk (1971). As shown in Figure 3, it consists of 16 spherical or cylindrical body parts, i.e.

head, neck, chest, abdomen, upper arms, lower arms, hands, thighs, legs and feet. Every body part except for chest has core, muscle, fat, skin, artery and vein nodes, while chest has heart, lung, core (bone), muscle, fat and skin nodes. In addition, each body part of upper and lower limbs has a superficial vein node as well. The artery and vein nodes are located at appropriate positions in each body part. Existence of the vessel nodes is the major difference between Stolwijk model and the present model.
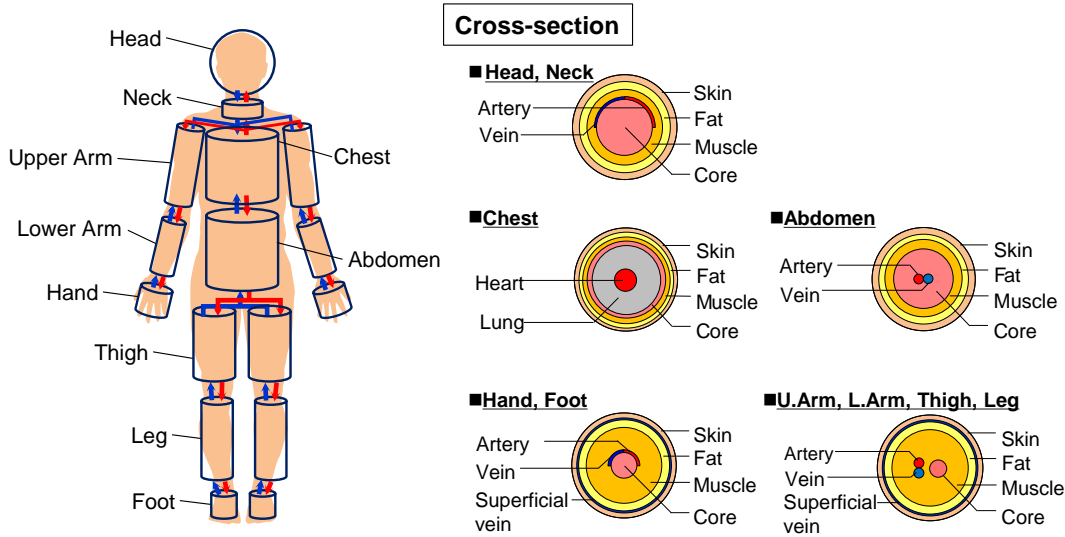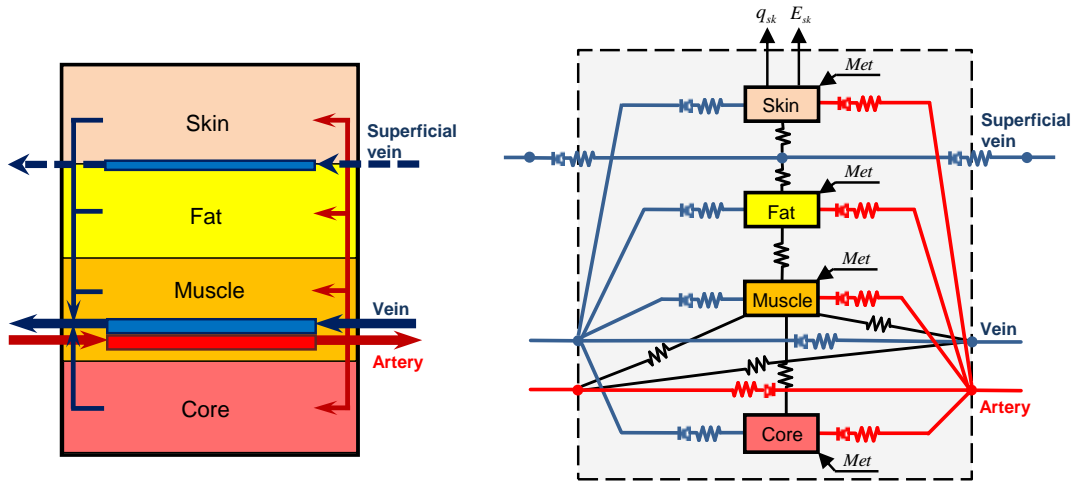
Figure 3. Schematic of thermal network model

Figure 4. Schematic of heat transfer at an example segment (Leg)

Figure 4 shows the schematic of heat transfer at leg as an example body part. Heat transfers between the artery and adjacent nodes are calculated by Equations (1) to (5), which are based on the same theory as heat exchangers in HVAC system.

$$q_1 = c\rho Q_{ar}\left\{1-\exp\left(-\frac{K_j S_j}{c\rho Q_{ar}}\right)\right\}\left(T_j - T_{ar,in}\right) \tag{1}$$

$$q_2 = c\rho Q_{ve}\phi\left(T_{ve,in} - T_{ar,in}\right) \tag{2}$$

$$\phi = \left[1-\exp\left\{-\frac{K_{ve}S_{ve}}{c\rho Q_{ve}}\left(1-\frac{Q_{ve}}{Q_{ar}}\right)\right\}\right]\bigg/\left[1-\frac{Q_{ve}}{Q_{ar}}\exp\left\{-\frac{K_{ve}S_{ve}}{c\rho Q_{ve}}\left(1-\frac{Q_{ve}}{Q_{ar}}\right)\right\}\right] \tag{3}$$

$$q_3 = c\rho Q_{ar} T_{ar,in} \tag{4}$$

$$q_4 = -c\rho Q_{ar} T_{ar,out} \tag{5}$$

Equation (1) expresses the heat exchange between the artery and adjacent tissue, i.e. the muscle node in case of leg. Equations (2) and (3) express the counter-flow heat exchange between the artery and vein. Equations (4) and (5) express the heat transfer due to the blood flow coming from the proximal node and leaving for the distal node, respectively. Thus, if we neglect time-derivative term as well as interaction of q_1 and q_2, the heat balance at the artery can be expressed as Equation (6).

$$q_1 + q_2 + q_3 + q_4 = 0 \tag{6}$$

Heat transfers of the vein are calculated in the similar manner, while those of the superficial vein were calculated in a different manner. The superficial vein is assumed to be a perfect mixing blood pool.

In order to validate this new thermal network model, numerical simulations were done regarding the same conditions as the subjective experiments. Measured values were provided for the input parameters as much as possible, because uncertainties other than the thermal network model should be minimized. Length, surface area and volume of each body part or node were derived from subject's MRI scan, and BFRs of respective body nodes were given by the experiments. Metabolic rates were determined with two methods. One was the measurement in the experiments. The other was the estimation from the volume of each tissue or organ and its basal metabolic rate per unit (Elia, 1992). The former method must be more accurate but could not determine the metabolic rate of each node. Therefore, the measured values were used as the whole body metabolic rates, and those were distributed to the respective body nodes in proportion to the estimated values by the latter method. On the other hand, the measured perspiration rates of whole body were distributed to the respective skin nodes in proportion to the surface areas.

3 RESULTS AND DISCUSSIONS
3.1 Subjective Experiments
Figure 5 shows the measured metabolic rate and estimated heat loss according to the measurements of skin heat flux and weight loss. The metabolic rate changed little due to ambient temperature, but the heat loss changed greatly. In addition, the heat losses in 18°C and 23°C cases were much higher than the metabolic rates, while those in the other cases were almost the same as the metabolic rates. This fact means that subjects' thermal conditions in 18°C and 23°C cases were not steady state, although we intended to measure under steady state conditions. This result was almost the same as the one reported by Gagge et al. (1938). According to the results by us and Gagge et al., thermoregulatory ability in cold environments is considered to be weaker than that in hot environments. From here, only the results of 28°C to 40°C cases are reported, because only these cases are steady state.

Figure 6 shows the cardiac output and its portions flowing into respective body parts. The portions were determined from the arterial BFR measurements and their mass balance, but those of neck and upper arms were exceptionally determined from estimated basal BFRs of muscle and fat and measured skin BFRs. This figure shows that the BFRs of limbs composed very small portions of total BFR, but they increased greatly with ambient temperature. On the other hand, the BFRs of head and trunk were large but changed only a little. As shown in Fig-

ure 7, the skin BFRs of limbs also increased more greatly than those of head and trunk. However, the change rates of skin BFRs at hand and foot were smaller than those of arterial BFRs at hand and foot. In the experiments, we used a skin BFR sensor which could measure only up to approx. 1 mm depth. Therefore, it is possible that blood flow through arteriovenous anastomoses (AVA) lying at deeper layer was not measured with this sensor.
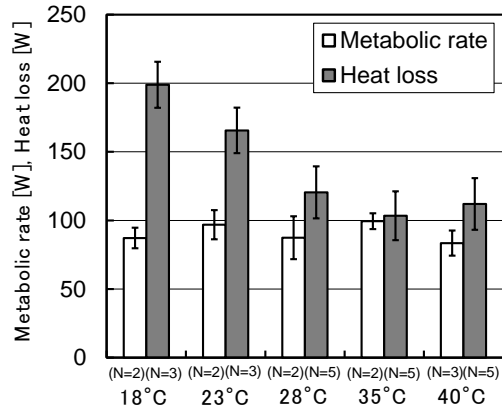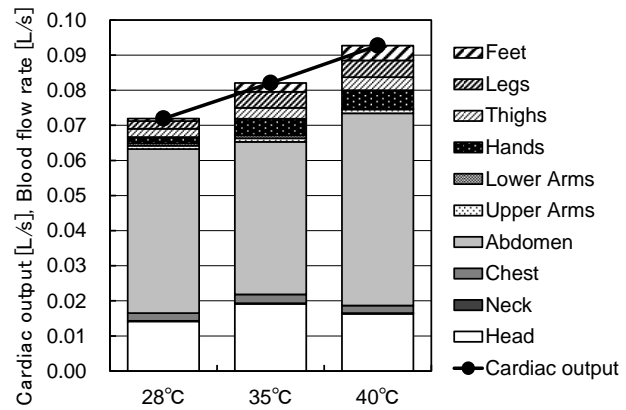

Figure 5. Metabolic rate and heat loss

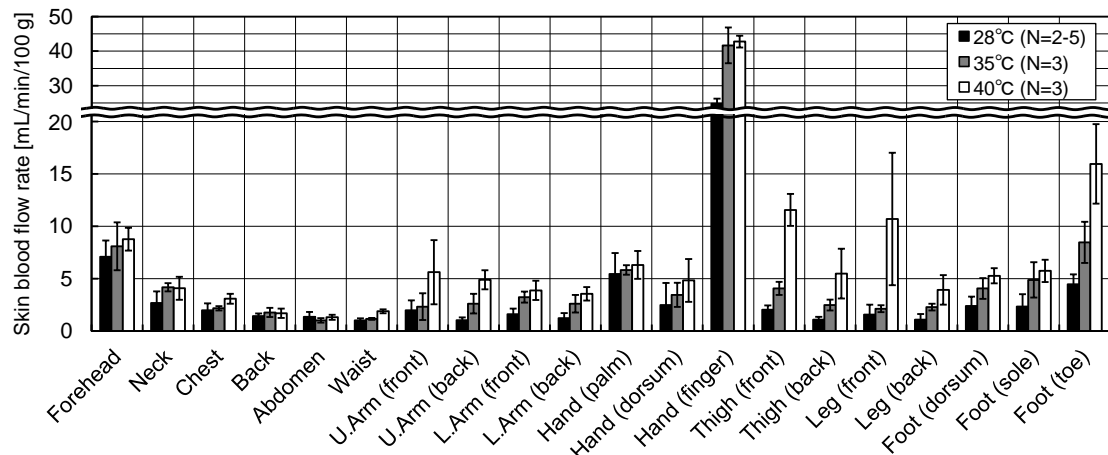Figure 6. Cardiac output and blood flow rates to respective body parts

Figure 7. Skin blood flow rates

3.2 Numerical Simulation

For the numerical simulations, BFRs to skin nodes were given as Figure 7, and those to fat nodes were given as basal BFRs estimated from their volumes. BFRs to core and muscle nodes were derived from BFRs of respective body parts (Figure 6). The portions of skin and fat were deducted from the BFR of each body part, and the rest was divided into core and muscle in proportion to their metabolic rates. Regarding hands and feet in 35°C and 40°C cases, the BFRs to core, muscle and fat were exceptionally fixed at the values in 28°C case, and the skin BFRs were given as the remaining BFRs after deduction of those values. Perspiration rates for the simulations were derived from the weight loss measurements as mentioned in 2.2. However, those in 40°C case were derived from sum of the measured metabolic rate and sensible heat loss, because unevaporated sweat was observed in this case.

Figure 8 shows the simulated tympanic and skin temperatures with comparing to the measurements. The simulated tympanic temperature was different up to 0.7°C, but the trend agreed reasonably. The simulated mean skin temperature was almost the same as the measurement,

while the local skin temperatures were different up to 2.5°C. The differences in local skin temperatures could be partly caused by rough estimation of local perspiration rates.

Figure 9 shows the result of an additional simulation in which BFRs in all cases were fixed at the ones in 28°C case. In this simulation, the simulated tympanic temperature was much higher than the measurement, while the simulated mean skin temperature was not different from the measurement. This result indicates that the BFRs of limbs are very important even if their portions are very small. Figure 10 shows the result of another simulation in which blood was directly exchanged between heart and each node in the same manner as Stolwijk model. The tympanic temperature simulated in this simulation was also much higher than the measurement. This result indicates the importance of heat transfer along the blood flow pathways.
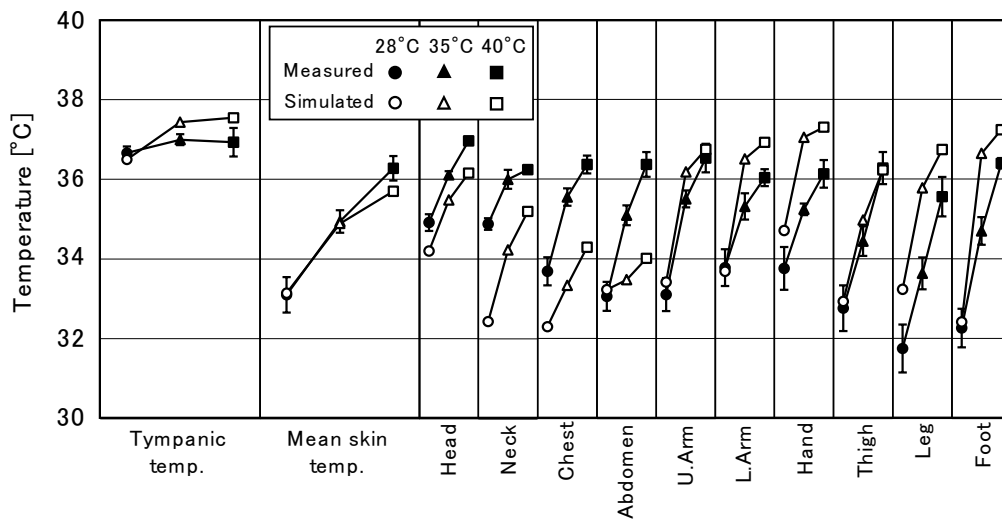

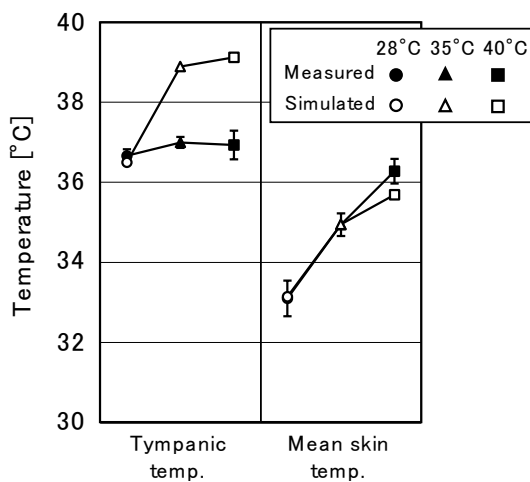Figure 8. Simulated tympanic temperature and skin temperatures

Figure 9. Simulated tympanic temperature and mean skin temperature without blood flow regulation
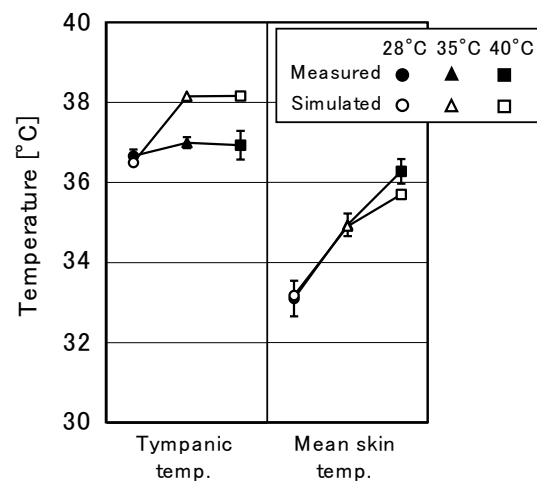
Figure 10. Simulated tympanic temperature and mean skin temperature without blood flow pathways

4 CONCLUSIONS

The subjective experiments indicated that human thermoregulatory ability in cold environments is weaker than that in hot environments. The experiments also showed that BFRs of limbs compose only small portions of total BFR but increase greatly with ambient temperature. On the other hand, our thermal network model could reproduce the trend of tympanic

temperature and mean skin temperature in the experiments. Moreover, the additional simulations showed that the BFRs of limbs are important for thermoregulation even if their portions are small, and besides, heat transfer along vessels is also important for thermoregulation.

ACKNOWLEDGEMENT

5 NOMENCLATURE

c: specific heat of blood [J/(kg·K)], E_{sk}: latent heat loss from skin surface [W], K: heat transmission coefficient [W/(m^2·K)], Met: metabolic heat [W], Q: blood flow rate [m^3/s], q: heat flow [W], q_{sk}: sensible heat loss from skin surface [W], S: contact area [m^2], T: temperature [°C], ϕ: temperature exchange efficiency [-], ρ: density [kg/m^3]

(Subscripts) ar: artery, j: adjacent node, in: entry side of vessel, out: exit side of vessel, sv: superficial vein, ve: vein

6 REFERENCES

Elia M. 1992. In: *Energy Metabolism, Tissue Determinants and Cellular Corollaries*. New York: Raven Press: 61-80.

Gagge AP, Winslow C-EA, Herrington LP. 1938. *American Journal of Physiology*, 124(1): 30-50

Goto T, Terayama D, Sugawara R, Sakamoto H. 2017. In: *Proceedings of Healthy Buildings Asia*, Tainan: 251-254.

Ministry of the environment government of Japan. 2014. *Environmental health manual of heat stroke* (in Japanese).

Sakamoto H, Chiba Y, Hayase T, Funamoto K, Saijo Y, Goto T. 2015. In: *Proceedings of Healthy Buildings Europe*, Eindhoven: ID437.

Stolwijk JAJ. 1971. *NASA contractor report*, NASA CR-1855.

Tokyo metropolitan institute of gerontology. 2013. *Reports of CPA patients in bath room in East Japan* (in Japanese).

Tochihara Y. 2012. *Journal of Snow Engineering of Japan*, 28(1): 37-40 (in Japanese).